JVI Journals.ASM.org

Arsenic Trioxide Stabilizes Accumulations of Adeno-Associated Virus Virions at the Perinuclear Region, Increasing Transduction *In Vitro* and *In Vivo*

Angela M. Mitchell,[a,b] Chengwen Li,[a,c] R. Jude Samulski[a,d]

Gene Therapy Center,[a] Department of Microbiology and Immunology,[b] Department of Pediatrics,[c] Department of Pharmacology,[d] University of North Carolina at Chapel Hill, Chapel Hill, North Carolina, USA

Interactions with cellular stress pathways are central to the life cycle of many latent viruses. Here, we utilize adeno-associated virus (AAV) as a model to study these interactions, as previous studies have demonstrated that cellular stressors frequently increase transduction of recombinant AAV (rAAV) vectors and may even substitute for helper virus functions. Since several chemotherapeutic drugs are known to increase rAAV transduction, we investigated the effect of arsenic trioxide (As_2O_3), an FDA-approved chemotherapeutic agent with known effects on several other virus life cycles, on the transduction of rAAV. *In vitro*, As_2O_3 caused a dose-dependent increase in rAAV2 transduction over a broad range of cell lines from various cell types and species (e.g., HEK-293, HeLa, HFF hTERT, C-12, and Cos-1). Mechanistically, As_2O_3 treatment acted to prevent loss of virions from the perinuclear region, which correlated with increased cellular vector genome retention, and was distinguishable from proteasome inhibition. To extend our investigation of the cellular mechanism, we inhibited reactive oxygen species formation and determined that the As_2O_3-mediated increase in rAAV2 transduction was dependent upon production of reactive oxygen species. To further validate our *in vitro* data, we tested the effect of As_2O_3 on rAAV transduction *in vivo* and determined that treatment initiated transgene expression as early as 2 days posttransduction and increased reporter expression by up to 10-fold. Moreover, the transduction of several other serotypes of rAAV was also enhanced *in vivo*, suggesting that As_2O_3 affects a pathway used by several AAV serotypes. In summary, our data support a model wherein As_2O_3 increases rAAV transduction both *in vitro* and *in vivo* and maintains perinuclear accumulations of capsids, facilitating productive nuclear trafficking.

Adeno-associated virus (AAV), a nonenveloped, single-stranded DNA virus, is a member of the family *Parvoviridae* and is classified as a dependovirus, as it requires the presence of a helper virus, such as adenovirus or herpes simplex virus (HSV), in order to replicate. In the absence of a helper virus, AAV's genome can persist episomally for long time periods (1). The AAV genome consists of two genes, *rep*, which encodes the nonstructural proteins, and *cap*, which encodes the capsid assembly protein and capsid proteins, flanked by inverted terminal repeats. To make recombinant AAV (rAAV) vectors, the two viral genes can be entirely removed from the genome with the terminal repeats being the only *cis* elements required for vector production (2), allowing for the examination of the viral transduction pathway leading up to gene expression. Although no pathogenesis has been linked to AAV, rAAV plays an important role as a gene delivery vector and is increasingly used for clinical gene therapy applications (reviewed in reference 3).

While there are several naturally occurring serotypes of AAV, the majority of AAV biology has been elucidated using rAAV serotype 2 (AAV2) vectors. rAAV2 is brought into cells through receptor-mediated endocytosis (4) and is trafficked through endosomal pathways, along microtubules, to the microtubule organizing center (MTOC) (5). rAAV2 then escapes from the endosome and is trafficked to the nucleus, where it uncoats (6), exposing the genome for second-strand synthesis and transcription. Several steps in the rAAV transduction pathway are inefficient, including nuclear entry (7) and second-strand synthesis (8, 9), and modifying the environment of the cell can lead to increased efficiency in these steps (6, 8). Specifically, several forms of cellular stress, including endoplasmic reticulum stress associated with unfolded protein responses (10), treatment with chemotherapeutic agents (6, 8), and heat shock (8, 11), have been shown to positively influence AAV transduction. In fact, our group was the first to demonstrate that heat shock, hydroxyurea, UV light, and X-rays are capable of increasing rAAV transduction through a mechanism involving the enhancement of second-strand DNA synthesis (8). Two of these treatments, hydroxyurea treatment and UV light in the presence of simian virus 40 (SV40) T antigen, were later shown to be able to substitute for helper virus functions and allow AAV replication in the absence of adenovirus (12). Moreover, dependence on stress responses in viral life cycles is not unique to AAV and has in fact been demonstrated to be important to the reactivation of many latent viruses, from lambda phage (13) to herpesviruses (14, 15). Although some stress response-dependent reactivation is due to dysregulation of the immune system (15), some may result from specific changes in the intracellular environment. In addition, the role of stress in the initial transduction of viruses other than AAV is less well understood than its role in latency.

The dependence of the AAV life cycle on cellular stress has been exploited to attempt to increase the efficiency of rAAV-mediated gene delivery and improve efficacy in clinical gene therapy appli-

Received 14 December 2012 **Accepted** 1 February 2013
Published ahead of print 13 February 2013
Address correspondence to R. Jude Samulski, rjs@med.unc.edu.

doi:10.1128/JVI.03443-12

cations. A number of chemotherapeutic agents have been used to induce cell stress and enhance rAAV transduction, including proteasome inhibitors such as MG-132, calpain inhibitor I, and bortezomib, DNA synthesis inhibitors such as hydroxyurea and aphidicolin, and topoisomerase inhibitors such as etoposide and camptothecin (6, 16–21). Thus far, the leading candidate for enhancing rAAV transduction *in vivo* is bortezomib, a proteasome inhibitor, which has been demonstrated to increase expression of a clinically relevant transgene 3- to 6-fold in a large-animal model (17). Although bortezomib is approved for use in humans, it has serious toxic side effects, and in rare cases its use can lead to liver failure and death (17, 22). Therefore, exploring the possibility of other, less toxic agents to enhance rAAV transduction *in vivo* remains an advantageous approach.

One specific cellular stressor that has not been examined for its effect on AAV biology is arsenic trioxide (As_2O_3). As_2O_3 was approved for the treatment of acute promyelocytic leukemia in 2000 (23) and is currently being evaluated for treatment of other forms of leukemia (24, 25). As_2O_3 is often considered to be a less toxic alternative to traditional chemotherapeutic agents. In fact, clinical studies have been published on the treatment of more than 1,100 promyelocytic leukemia patients with As_2O_3 (26), and the side effects of the current course of treatment (5 weeks of daily doses) are relatively mild, including dermatological issues, fatigue, and nausea. A comparatively severe cardiac side effect is prolonged QT interval; however, this effect is reversible after treatment ceases and has not led to any As_2O_3-associated deaths (25). Furthermore, oral preparations of As_2O_3 are being investigated and appear to avoid this complication (23). These clinical features make As_2O_3 a promising stressor to consider for use in enhancing rAAV transduction.

Numerous studies have worked to define the mechanisms by which As_2O_3 acts to treat promyelocytic leukemia. When cells are treated with As_2O_3, it is taken up through aquaglyceroporins and then acts on a molecular level by binding thiol ligands from cysteine residues (27). On a cellular level, As_2O_3 has many effects, including inducing reactive oxygen species (ROS) formation (28), inhibiting NF-κB activation (29), degrading the promyelocytic leukemia protein (PML) (30), changing mitochondrial membrane potentials (31), inducing global changes in transcriptional patterns (32), and, at high doses, inducing apoptosis (24, 33). Therefore, As_2O_3 can lead to widespread changes in the cellular environment. In addition, As_2O_3 has previously been demonstrated to have effects on several different viruses. Specifically, As_2O_3 increases human immunodeficiency virus (HIV) infection in nonpermissive cell types but has no effect in permissive cell types (34–36). Moreover, treatment of patients with As_2O_3 often leads to the reactivation of varicella-zoster virus (VZV) and HSV (37, 38); in fact, the risk of patients developing herpes zoster after As_2O_3 treatment is 26%, which is higher than the 20% risk found with severe immunosuppression after hematopoietic stem cell transplant (37). Indeed, the high rate of herpes reactivation has led some groups to proscribe prophylactic acyclovir during As_2O_3 treatment (23).

As As_2O_3 affects these other viruses, and chemotherapeutic agents, such as proteasome inhibitors (6, 39) and topoisomerase inhibitors (18), have been demonstrated to enhance rAAV transduction, we determined whether As_2O_3 has an effect on initial rAAV transduction. We utilized rAAV2 vectors and examined transduction both in As_2O_3-treated cells and *in vivo*. We determined that transduction of rAAV2 was enhanced *in vitro* and *in vivo*, and that the transduction of several different rAAV serotypes was also enhanced *in vivo*. In addition, we determined that As_2O_3 treatment of cells maintained the accumulation of rAAV2 virions at the MTOC, and that this effect was dependent on induction of ROS formation. The enhancement of rAAV transduction by As_2O_3 and the mechanisms behind this enhancement have implications for the enhancement of rAAV-mediated gene delivery and possibly for the initial infection pathways of other viruses affected by As_2O_3.

MATERIALS AND METHODS

Cell culture and chemicals. HEK-293 cells, HeLa cells, human foreskin fibroblasts immortalized with telomerase (HFF hTERT), and Cos-1 cells were maintained in Dulbecco's modified Eagle medium (DMEM). C-12 cells were maintained in minimal essential medium (MEM) alpha without ribonucleosides and deoxyribonucleosides, and Cho-K1 cells were maintained in Ham's F-12 medium. Cells utilized in confocal microscopy experiments were maintained in MEM without phenol red and were supplemented with 2 mM L-glutamine and 1× MEM nonessential amino acids for at least two passages before imaging. All cells were maintained at 37°C and 5% CO_2, and medium was supplemented with 10% fetal bovine serum, 100 U/ml penicillin, and 100 g/ml streptomycin.

As_2O_3 (Sigma-Aldrich) was prepared for *in vitro* use as a 1 mM solution in 200 mM NaOH and compared to a vehicle control of the same pH. For *in vivo* use, a 50 mg/ml solution of As_2O_3 in 1 M NaOH was prepared, diluted to 0.5 mg/ml in phosphate-buffered saline (PBS), and brought to a neutral pH with HCl. A proteasome inhibitor, MG-132 (Calbiochem), was prepared at 10 mM in dimethylsulfoxide (DMSO). N-acetyl-L-cysteine (NAC; Sigma-Aldrich) was prepared at 500 mM in PBS. Dihydroethidium (DHE; Sigma-Aldrich) was prepared at 10 mM in DMSO.

Virus production. rAAV vector was produced in HEK-293 cells as previously described (40). Briefly, rAAV was prepared by transfection of HEK-293 cells with pXX680, a pXR plasmid (pXR2, pXR6, pXR8, or pXR9 for the different serotypes of rAAV produced), and either pTR-CBA-EGFP or pTR-CBA-Luc. After 48 h, cells were harvested, lysed, and DNase treated. For general use, vector was purified on a cesium chloride gradient and then dialyzed to remove the cesium. To produce pure vector for fluorescent labeling, the vector was purified on a discontinuous iodixanol gradient followed by ion-exchange chromatography and dialysis. The titers of the vectors were determined by quantitative PCR (qPCR) as previously described (40).

Transduction assays. For transduction experiments, 8×10^4 cells were seeded per well of a 24-well plate 16 to 18 h prior to transduction and, where indicated, were treated with the stated doses of As_2O_3 or vehicle control at the time of seeding. Vector was added in fresh media at the indicated vector dose. For proteasome inhibition experiments, 1 μM MG132 or a DMSO control was added concurrently with transduction. Cells were harvested by trypsinization at 48 h posttransduction unless otherwise noted. For flow cytometry, trypsinized cells were resuspended in 2% paraformaldehyde and analyzed using a Beckman-Coulter CyAn ADP instrument. Enhanced green fluorescent protein (EGFP) fluorescence was measured using a 488-nm excitation laser and 530- to 540-nm emission filter.

DNA purification and qPCR of viral genome copy number. For quantification of intracellular vector genome copies (vg), transduced cells were harvested by trypsinization and washed with PBS, and total DNA was harvested using the Qiagen DNeasy blood and tissue kit per the manufacturer's instructions. Viral genomes and cellular endogenous control genes were quantified as previously described (6). Briefly, primers were utilized to quantitate EGFP (forward, 5′-AGC AGC ACG ACT TCT TCA AGT CC-3′; reverse, 5′-TGT AGT TGT ACT CCA GCT TGT GCC-3′), luciferase (forward, 5′-AAA AGC ACT CTG ATT GAC AAA TAC3′; reverse, 5′-CCT TCG CTT CAA AAA ATG GAA C-3′), human LB2C1 (forward, 5′-GTT AAC AGT CAG GCG CAT GGG CC-3′; reverse, 5′-CCA TCA

GGG TCA CCT CTG GTT CC-3′), mouse β-actin (forward, 5′-TGG CAC CAC ACC TTC TAC AAT-3′; reverse, 5′-AGG CAT ACA GGG ACA GCA CA-3′), and hamster glyceraldehyde-3-phosphate dehydrogenase (GAPDH) (forward, 5′-CGT ATT GGA CGC CTG GTT AC-3′; reverse, 5′-GGC AAC AAC TTC CAC TTT GC-3′). The human LB2C1 primer set was also used to quantitate Cos-1 cellular genomes. All reactions were run with Sybr Green master mix (Roche Applied Sciences) on a Roche LightCycler 480. The following run protocol was used: 95°C for 10 min, followed by 45 cycles of 95°C for 10 s, 60°C for 10 s, and 72°C for 10 s. Absolute quantification was performed based on second-derivative maximum comparisons to standard curves of plasmid DNA (EGFP and luciferase) or untransduced cellular DNA.

Cell cycle analysis. For analysis of the proportion of cells in each stage of the cell cycle, cells were treated overnight with As_2O_3 as described for transduction assays and then harvested at the conclusion of As_2O_3 treatment. Propidium iodide staining was performed as has been previously described (41), with slight modifications. Briefly, cells were washed twice with PBS plus 0.1% fetal bovine serum and then fixed in ethanol overnight. After fixation, cells were washed and then resuspended in propidium iodide staining solution (40 μg/ml propidium iodide [Sigma-Aldrich] in PBS with 3.8 mM sodium citrate) and 0.5 μg RNase A (Sigma-Aldrich) and allowed to stain for at least 3 h at 4°C. DNA content was analyzed by flow cytometry at a low rate of flow. Flow cytometry was performed on a Beckman-Coulter CyAn ADP instrument using a 488-nm excitation laser and a 613- to 620-nm emission filter.

Capsid labeling and confocal microscopy. rAAV2 virions were fluorescently labeled with Cy5 and used for confocal imaging as previously described (42), with slight modifications. Briefly, pure rAAV2 virions were incubated with 5,000 molecules of mono-NHS-Cy5 (GE Healthcare) per vector genome for 45 min at room temperature and then extensively dialyzed to remove excess dye. The titer of the labeled vector was determined by qPCR. For confocal imaging experiments, Cho-K1 cells were seeded and treated with As_2O_3 as described for transduction experiments on poly-L-lysine-coated coverslips. Cy5-labeled rAAV2 was added to the cells at 10,000 vg/cell 16 to 18 h after seeding. At the time of harvest, cells were washed three times with PBS, fixed with 2% paraformaldehyde for 15 min at room temperature, washed 2 times with PBS and 1 time with double-distilled H_2O, and mounted on slides with ProLong Gold Antifade Reagent with 4′,6-diamidino-2-phenylindole (DAPI) (Molecular Probes).

For confocal microscopy, rAAV2 virion localization was analyzed with a Zeiss LSM 710 spectral confocal laser-scanning microscope using a Plan Apochromat 63×/1.40-numerical-aperture oil objective. Z stacks of 12 to 14 focal planes were acquired at 0.63-μm Z intervals, and these images were used to create three-dimensional (3D) reconstructions. Images were deconvoluted using the AutoQuant X3 program (MediaCybernetics) to perform 3D blind adaptive point spread function deconvolution. The IMARIS software package (Bitplane AG) was used to create 3D projections of the stacks.

Reactive oxygen species quantification and scavenging. Cells were seeded and treated as described for transduction experiments. For ROS scavenging experiments, NAC was added to cells at the indicated doses at the time of As_2O_3 treatment. NAC and As_2O_3 were removed at the time of transduction, and transduction was assayed as described above. Quantification of ROS levels by DHE staining has been previously described (43). Briefly, cells were harvested by trypsinization 16 to 18 h after treatment, washed twice with PBS, and then incubated for 30 min at 37°C in 10 μM DHE in PBS. After incubation, the cells were washed once with PBS. Flow cytometry was performed on the Beckman-Coulter CyAn ADP instrument using a 488-nm excitation laser and a 575- to 625-nm emission filter.

***In vivo* transduction assays.** All mouse experiments were conducted in accordance with the policies of the University of North Carolina at Chapel Hill's Institutional Animal Care and Use Committee. For *in vivo* transduction experiments, age- and strain-matched female mice (Jackson Laboratories) were treated with 5 μg/g/day As_2O_3 or a PBS vehicle control by intraperitoneal (i.p.) injection for 5 days. On the third day of treatment, mice were transduced with the indicated dose of AAV vector in PBS by retro-orbital injection. Live imaging of luciferase expression from AAV vectors has been previously described (44). Briefly, mice were given 150 mg/kg D-luciferin (Caliper LifeSciences) by i.p. injection, and after 5 min, luminescence was measured using the IVIS-Lumina imaging system (Caliper LifeSciences). The Igor Pro 3.0 software was used to quantitate luminescence signals.

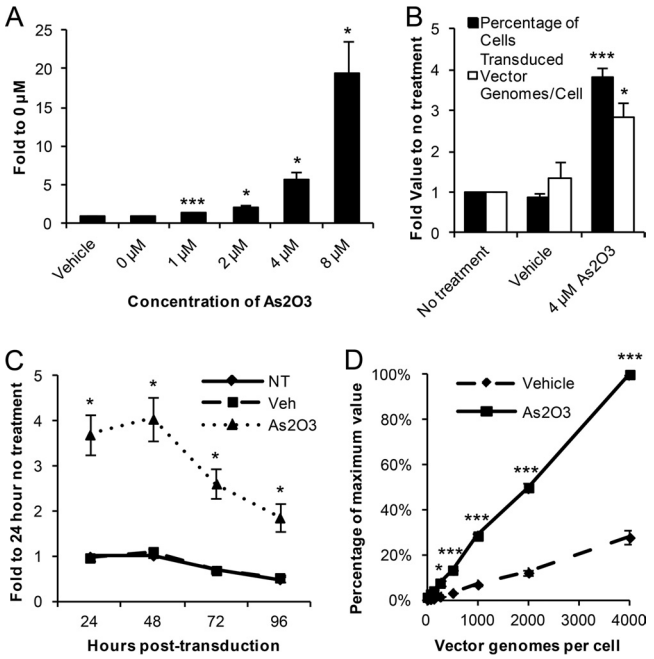

FIG 1 HEK-293 cells transduced by rAAV2 after As_2O_3 treatment. HEK-293 cells were treated overnight with As_2O_3 or a vehicle control and then transduced with rAAV2-CBA-EGFP. (A) Cells were treated with the indicated dose of As_2O_3 and transduced with 500 vg/cell rAAV2. The percentage of cells transduced at 48 h posttransduction is shown as the fold increase compared to the level for the no-treatment group. (B) The numbers of vector genome copies per cell present and percentages of cells transduced were assayed at 48 h posttransduction following the indicated treatment and transduction with 500 vg/cell. Values are indicated as fold increase compared to results for the no-treatment group. (C) Cells were treated and transduced as described for panel B, harvested at the indicated time points, and assayed for the percentage of cells transduced. Values are indicated as fold increase compared to the no-treatment group at 24 h. NT, no treatment; Veh, vehicle. (D) After treatment as described for panel B, cells were transduced with the indicated doses of rAAV2, and the percentage of cells transduced was assayed 48 h posttransduction. Values represent the percentage of the maximum value reached in each experiment. Data shown are the means from at least 3 independent experiments; error bars represent the standard errors of the means (SEM). $P < 0.05$ (*) and $P < 0.005$ (***) based on comparisons of sample means by the Student *t* test.

RESULTS

Arsenic trioxide treatment increases the percentage of cells transduced with rAAV2. To expand our knowledge of AAV's responses to cellular stressors, we set out to determine whether As_2O_3 treatment had an effect on rAAV2's initial transduction. We first treated HEK-293 cells overnight with various doses of As_2O_3, transduced them with rAAV2-EGFP, and assayed the percentage of cells transduced after 48 h. After As_2O_3 treatment, we observed a dose-dependent increase in the percentage of cells transduced by rAAV2 (Fig. 1A), with a maximum increase of 19.4-fold in the 8 μM As_2O_3 group. Due to toxicity from higher As_2O_3

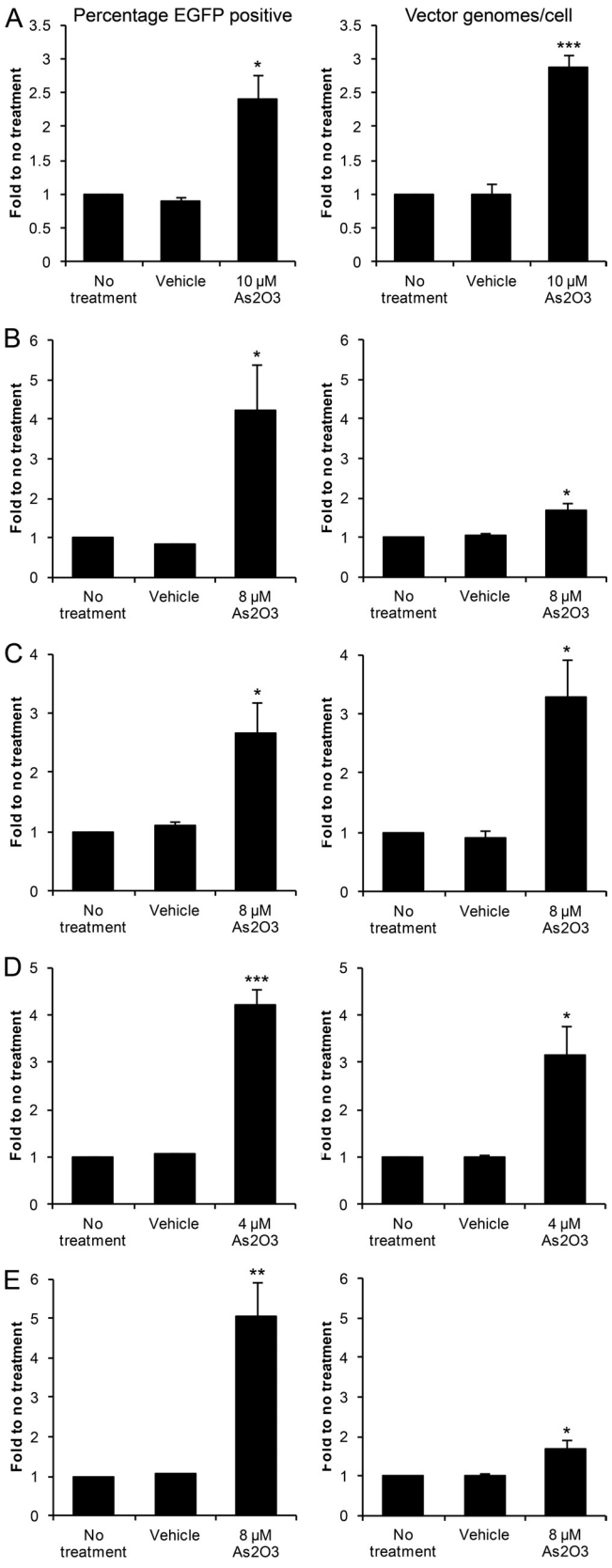

FIG 2 rAAV2 transduction after As_2O_3 treatment of several human and nonhuman cell lines. Cells were treated overnight with the indicated doses of As_2O_3 and a cell line-specific dose of rAAV2. The percentage of cells transduced (left) and numbers of vector genomes per cell (right) were assayed 48 h posttransduction in HeLa cells transduced with 250 vg/cell (A), HFF hTERT transduced with 5,000 vg/cell (B), Cos-1 cells transduced with 1,000 vg/cell (C), C-12 cells transduced with 3,000 vg/cell (D), and Cho-K1 cells transduced with 5,000 vg/cell (E). Values represent the fold change compared to results for no treatment and are the means from at least 3 independent experiments. Error bars represent the SEM. $P < 0.05$ (*), $P < 0.01$ (**), and $P < 0.005$ (***) based on comparisons of sample means by the Student *t* test.

concentrations (data not shown), further experiments were conducted in HEK-293 cells with the 4 μM As_2O_3 dose to verify that the increase in the percentage of cells transduced observed with As_2O_3 treatment was due to an increase in transduction and not an increase in transgene expression. We assayed the numbers of vector genomes present in the cells 48 h posttransduction and determined that the increase in the intracellular vector genome copy number correlated very well with the percentage of cells transduced (Fig. 1B). In addition, we observed no increase in transgene expression from a plasmid carrying the transgene cassette following As_2O_3 treatment (data not shown). To determine whether As_2O_3's transduction effect is stable over time, we treated the cells as described above, assayed transduction from 24 to 96 h posttransduction, and determined that As_2O_3 increased transduction to a similar extent at all of the time points assayed (Fig. 1C). Furthermore, we also investigated whether the effect of As_2O_3 would be maintained at a range of vector doses. In fact, we observed significant increases in transduction with As_2O_3 treatment with rAAV2 doses from 250 to 4,000 vg/cell (Fig. 1D). The increase in the numbers of vector genomes per cell in both the vehicle-treated and As_2O_3-treated cells was linear (R^2 values of 0.996 and 0.999, respectively).

The effects of As_2O_3 treatment on HIV infection can only be observed in nonpermissive cell types (34–36); therefore, given the increase in rAAV2 transduction observed with As_2O_3 treatment in HEK-293 cells, we tested the effect of As_2O_3 in other human and nonhuman cell lines. We optimized rAAV2 doses to result in 5 to 10% of cells transduced without treatment and performed dose curves to identify doses of As_2O_3 capable of increasing rAAV2 transduction without overt toxicity (data not shown), as sensitivity of cells to As_2O_3 varies based on cellular glutathione levels (28). In HeLa cells, which have been commonly utilized as a model cell line for exploring AAV biology, we observed a 2.4-fold increase in AAV2 transduction following As_2O_3 treatment that correlated well with an increase in the vector genome copy number (Fig. 2A). We then investigated a human diploid cell line, HFF hTERT. In these cells, we observed a 4.2-fold increase in the percentage of cells transduced with rAAV2; however, the increase in the vector genome copy number was smaller, although it was still significant (Fig. 2B).

To determine whether the effect of As_2O_3 on rAAV2 transduction is restricted to human cells, we investigated the effect of As_2O_3 in several nonhuman cell lines. In Cos-1 cells, which are of nonhuman primate origin, we observed a 2.7-fold increase in the percentage of cells transduced that correlated well with an increase in the vector genome copy number (Fig. 2C). As rAAV2 is liver tropic, we next investigated the effect of As_2O_3 on transduction of a mouse hepatoma-derived cell line, C-12. As_2O_3 treatment increased the percentage of cells transduced with rAAV2 by 4.2-fold in this cell line, and this increase correlated well with the increase in the vector genome copy number (Fig. 2D). Finally, we tested the

effect of As_2O_3 in Cho-K1 cells, which are hamster cells with normal protein modification pathways, and observed a 5.0-fold increase in the percentage of cells transduced with As_2O_3 treatment, although the increase in the vector genome copy number was smaller (Fig. 2E). Therefore, the increase in transduction observed after As_2O_3 treatment is not restricted to a specific cell type or to a specific species origin.

Arsenic trioxide acts in the first 24 h of transduction through a postentry mechanism. To gain mechanistic insights into the actions of As_2O_3 on rAAV2 transduction, we first examined the effect of As_2O_3 on self-complementary rAAV2 transduction, which does not require second-strand DNA synthesis. We determined that As_2O_3 caused a similar increase in rAAV transduction with both single-stranded (ssAAV) and self-complementary (scAAV) rAAV, suggesting that As_2O_3 affects a step in rAAV transduction prior to second-strand synthesis (Fig. 3A). To determine when this effect occurs, we investigated the effect of the timing of As_2O_3 addition on the transduction of rAAV2. We treated cells with As_2O_3 from 18 h before transduction or 0, 3, 7, or 24 h posttransduction to the time of harvest and assayed the percentage of cells transduced with rAAV2. We observed that the majority of the As_2O_3 effect was confined to pretreatment and treatment within the first 24 h of transduction (Fig. 3B). Since As_2O_3 acts in the first 24 h of transduction (Fig. 3B) and the vector genome copy number is increased similarly to the percentage of cells transduced at 48 h posttransduction (Fig. 1B), we then investigated the change in numbers of intracellular vector genomes over time. The vector genome copy number was similar between As_2O_3- and vehicle-treated cells until 15 to 18 h posttransduction; however, vector genome copy number in the vehicle-treated cells then decreased at a higher rate than that of As_2O_3-treated cells (Fig. 3C). The difference in the percentage of cells transduced at each time point correlated well with the difference in the vector genome copy numbers (data not shown). These data suggest that the effect of As_2O_3 occurs after rAAV2 has entered the cell and prior to second-strand DNA synthesis. To determine whether the increase in rAAV vector genome copy number or transduction is due to inhibition of the cell cycle following As_2O_3 treatment, we treated cells overnight with As_2O_3 or a vehicle control and then measured the proportion of cells in each stage of the cell cycle. We determined that there was very little or no change in the percentage of cells in each cell cycle stage following As_2O_3 treatment (Fig. 3D), and that any changes were within the range of variability between experiments. These data are substantiated by our toxicity assays, in which equal numbers of total and viable cells were observed following As_2O_3 treatment (data not shown). Given these data, it is unlikely that the 3- to 4-fold changes in rAAV transduction and vector genome copy number could result from a decrease in cell division rates. Therefore, these data suggest that the increase in vector genome copy number and in rAAV transduction is not due to cell cycle arrest but instead is due to another change in the intracellular environment.

Increased vector copy number is also observed with proteasome inhibition of AAV-transduced cells, which induces the nucleolar localization of rAAV2 (6); therefore, we investigated whether the effects of proteasome inhibition and As_2O_3 treatment on AAV2 transduction overlap. When cells were pretreated with As_2O_3 and then cotreated with a proteasome inhibitor, MG132, and rAAV2, there was no additional increase in the percentage of cells transduced between MG132 treatment and MG132/As_2O_3 treatment. However, the median fluorescence intensity (MFI) of the positive cells was greater for the combined MG132/As_2O_3 treatment than for MG132 alone (Fig. 3E). As both of these drugs appear to act through postentry mechanisms, this suggests that the combination of the drugs leads to more successful intracellular trafficking despite the lack of increase in the numbers of cells transduced when the drugs were combined; nevertheless, the additional increase in the MFI with MG132 and As_2O_3 treatment

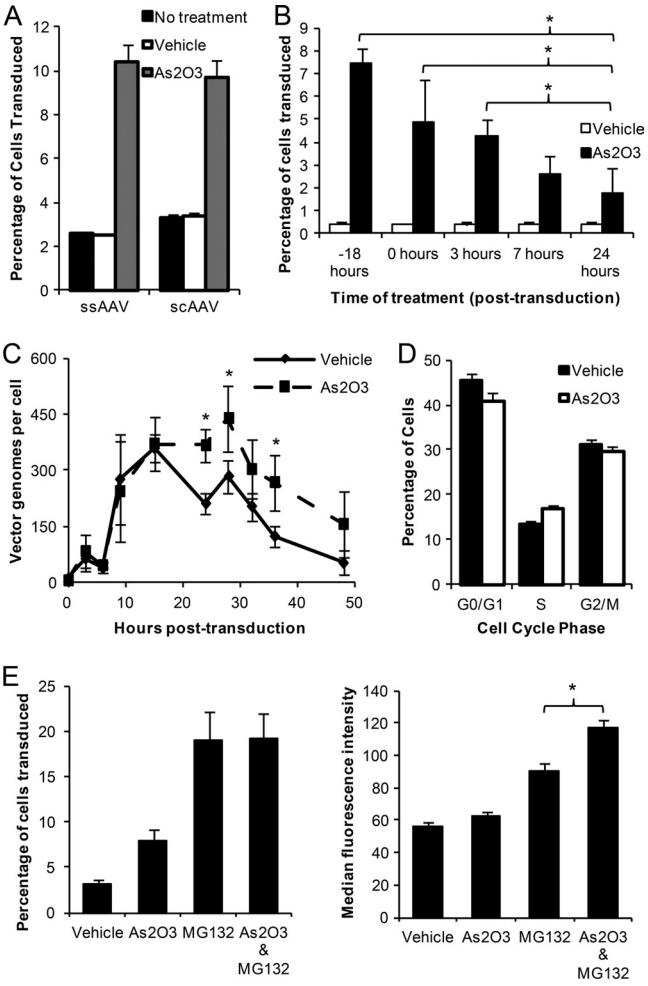

FIG 3 Mechanistic insights regarding rAAV2 transduction after As_2O_3 treatment. (A) HEK-293 cells were treated overnight with 4 μM As_2O_3 or a vehicle control and then transduced with 500 vg/cell single-stranded rAAV2 (ssAAV) or 100 vg/cell self-complementary rAAV2 (scAAV), and the percentage of cells transduced was assayed at 48 h posttransduction. (B) HEK-293 cells were treated with 4 μM As_2O_3 or a vehicle control starting at the indicated times and continuing to the time of harvest, 48 h posttransduction with 500 vg/cell rAAV2, and the percentage of cells transduced was assayed. (C) HEK-293 cells were treated overnight with 4 μM As_2O_3 or vehicle and then transduced with 1,000 vg/cell rAAV2, and numbers of intracellular vector genomes were assayed at the indicated times posttransduction. (D) HEK-293 cells were treated overnight with 4 μM As_2O_3 or a vehicle control and then stained with propidium iodide to determine the percentage of cells in each cell cycle stage. (E) HEK-293 cells were treated as described for panel C, and 1 μM MG132, a proteasome inhibitor, or a vehicle control was added at the time of transduction. Cells were harvested at 24 h posttransduction, and the percentage of GFP-positive cells and the median fluorescence intensity of the positive cells were assayed. Data representative of three independent experiments is shown. Error bars represent 1 standard deviation (SD). *, $P < 0.05$ based on the nonparametric Kruskal-Wallis test.

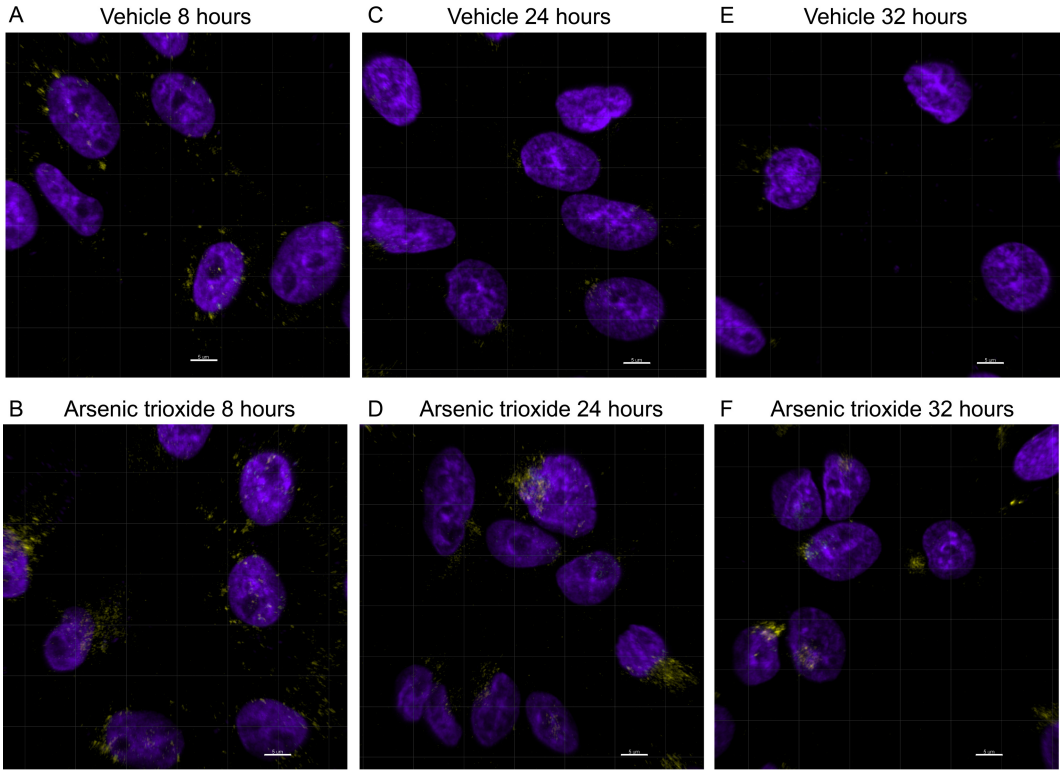

FIG 4 Subcellular localization of rAAV2-Cy5 virions after As_2O_3 treatment. Cho-K1 cells were treated with a vehicle control (A, C, and E) or 8 μM As_2O_3 (B, D, and F) from 18 h pretransduction to the time of harvest and were transduced with 10,000 vg/cell rAAV2-Cy5. Cells were fixed at 8 h posttransduction (A and B), 24 h posttransduction (C and D), or 32 h posttransduction (E and F). The localization of rAAV virions was determined by confocal microscopy, and representative deconvoluted 3D projections are shown. Cy5 signal is shown in yellow; DAPI signal is shown in purple. Scale bars represent 5 μm.

suggests at least partially independent mechanisms for these two drugs.

Arsenic trioxide treatment stabilizes accumulations of rAAV2 virions over time and acts through reactive oxygen species formation. To determine whether the lower rate of vector genome loss we observed occurred on the level of the virion or on the level of the genome, we transduced Cho-K1 cells, which are amenable to imaging techniques, with fluorescently labeled rAAV2 virions and tracked their intracellular trafficking through confocal microscopy after either vehicle treatment or As_2O_3 pre- and cotreatment. Previous observations have suggested that rAAV traffics to the perinuclear region on microtubules where it accumulates, and then some portion of virions proceed to the nucleus, where uncoating occurs (5, 6, 45). At 8 h posttransduction, a time at which the vector genome copy number was similar between vehicle- and arsenic-treated HEK-293 cells (Fig. 3A), we observed very little difference in the localization of virions between the vehicle-treated (Fig. 4A) and As_2O_3-treated (Fig. 4B) cells. However, at 24 h posttransduction, although we observed some perinuclear accumulation of virions with vehicle treatment (Fig. 4C), much larger perinuclear accumulations of virions were present in As_2O_3-treated cells (Fig. 4D). This effect was even more pronounced at 32 h posttransduction, when many vehicle-treated cells had few or no AAV virions remaining (Fig. 4E), but As_2O_3-treated cells still had large, condensed perinuclear accumulations of virions (Fig. 4F). We observed no clear differences in the amount or localization of intact virions in the nucleus at any of these time points. Together, these data suggest that As_2O_3 prevents the loss of intracellular rAAV2 virions during transduction.

Many cellular effects of As_2O_3 are mediated through the formation of ROS (reviewed in reference 46). Consequently, we investigated whether the effect of As_2O_3 on rAAV2 transduction was mediated by ROS formation. When cells were treated with increasing doses of As_2O_3, we observed a dose-dependent increase in the levels of intracellular ROS, as evidenced by increased red fluorescence following DHE staining of treated cells (Fig. 5A). Specifically, significant increases in the MFI were observed with the 2, 4, and 8 μM As_2O_3 treatments (Fig. 5C). As the dose-dependent increase in ROS mirrors the dose-dependent increase in AAV2 transduction following As_2O_3 treatment, we then investigated whether inhibiting ROS formation, by treating cells with N-acetyl-L-cysteine (NAC), would inhibit the transduction effects of As_2O_3. We treated cells overnight with As_2O_3 and NAC, transduced them with rAAV2, and measured the levels of ROS present at the time of transduction and the percentage of cells transduced 48 h posttransduction. Although treatment with As_2O_3 induced ROS formation, treatment with NAC caused a dose-dependent decrease in ROS formation, where 10 mM NAC treatment of As_2O_3-treated cells resulted in a population that overlaid that of the vehicle control (Fig. 5B). When we assayed for transduction, we observed a dose-dependent decrease in transduction following NAC and As_2O_3 cotreatment compared to treatment with As_2O_3 alone (Fig. 5D). NAC had no effect on the transduction of vehicle-treated cells. These data suggest that As_2O_3 acts through the for-

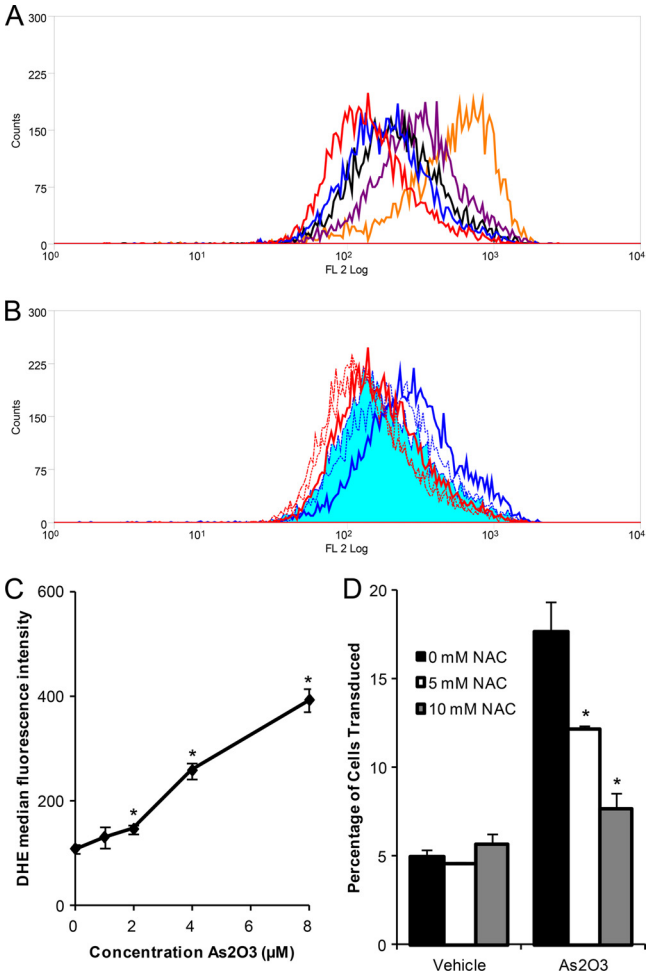

FIG 5 Role of ROS in the rAAV2 transduction effects of As_2O_3. (A) HEK-293 cells were treated overnight with no treatment (red), 1 μM As_2O_3 (blue), 2 μM As_2O_3 (black), 4 μM As_2O_3 (purple), or 8 μM As_2O_3 (orange), and ROS were measured with DHE. A histogram of fluorescence intensity is shown. (B) HEK-293 cells were treated overnight with a vehicle control (red) or 4 μM As_2O_3 (blue) and with PBS (solid line), 5 mM NAC (small dashed line), or 10 mM NAC (intermediate dashed line) to scavenge ROS. ROS were measured with DHE, and a histogram of fluorescence intensity is shown. The curve representing As_2O_3 ad 10 mM NAC treatment is shaded solid blue in the histogram. (C) Cells were treated as described for panel A, and the median fluorescence intensity was plotted versus As_2O_3 concentration. (D) Cells were treated as described for panel B and then transduced with 500 vg/cell rAAV2, and the percentage of cells transduced was assayed at 48 h posttransduction. Data are representative of three independent experiments. Error bars represent 1 SD. *, $P < 0.05$ based on the Kruskal-Wallis test.

mation of ROS, leading to a decrease in the loss of rAAV2 virions over time and, thus, to increased AAV transduction.

Arsenic trioxide increases rAAV2 transduction *in vivo* but does not change tropism. To determine whether the increase in rAAV2 transduction we observed with As_2O_3 *in vitro* could be replicated *in vivo*, we treated mice for 5 days with a dose of 5 μg/g/day As_2O_3, which replicates the levels of serum As_2O_3 observed in promyelocytic leukemia patients treated with this drug (47, 48). With this dose of As_2O_3, we observed no weight loss or overt toxicity and no increase in serum liver enzyme levels (alanine aminotransferase [ALT] and aspartate aminotransferase [AST]) over those of the vehicle control, suggesting a lack of acute liver toxicity (data not shown). We transduced mice systemically with 2×10^{11} vg rAAV2-luciferase on the third day of As_2O_3 treatment and measured transduction through luciferase live imaging. We observed measurable luciferase activity in As_2O_3-treated mice as early as 2 days posttransduction, at which time the activity of vehicle-treated mice was close to background levels (Fig. 6A). By day 7 posttransduction, all As_2O_3-treated mice were expressing strongly, while the vehicle-treated mice were showing early, low levels of expression (Fig. 6B). Furthermore, when we quantified expression in the whole mouse (Fig. 6C) or the area of the liver alone (Fig. 6D), we observed significant increases in transduction at 5 to 12 days posttransduction. In fact, at day 5 posttransduction, liver expression in As_2O_3-treated mice was 19.3-fold greater than that of the vehicle-treated mice (Fig. 6D). These data suggest that As_2O_3 can increase rAAV2 transduction *in vivo*. To confirm the increased expression observed in our live imaging data, we harvested the organs from mice at 14 days posttransduction and performed biodistribution experiments. In the liver, we observed a 3.8-fold increase in normalized luciferase activity with As_2O_3 treatment and minimal expression in the other organs tested (data not shown). Furthermore, analysis of vector genome copy numbers suggested no changes in vector tropism due to As_2O_3 treatment (data not shown). These data suggest that As_2O_3 can increase rAAV2 transduction *in vivo* without altering vector tropism.

Arsenic trioxide increases the transduction of several serotypes of AAV *in vivo*. To determine whether As_2O_3's effect is specific to rAAV2 or can be applied to other rAAV serotypes, we treated mice with As_2O_3 as before, transduced them with 1×10^{11} vg rAAV6, rAAV8, or rAAV9, and assayed transduction by luciferase live imaging. With rAAV6, we observed a clear increase in transduction at day 7 posttransduction (Fig. 7A), which could also be observed at 14 days posttransduction (data not shown). Quantification of this increase demonstrated a 5.5-fold enhancement at day 7 (Fig. 7B). With rAAV8, we observed an enhancement of transduction from As_2O_3 treatment at day 2 posttransduction (Fig. 7C), which was quantified at 3.0-fold (Fig. 7C); however, this enhancement was not observed at later time points (data not shown). Finally, with rAAV9, we observed an enhancement of transduction at day 5 posttransduction (Fig. 7E), which was quantified at 4.2-fold (Fig. 7F). In fact, As_2O_3 enhanced in rAAV9 transduction from 2 days posttransduction through 3 weeks posttransduction (Fig. 7G and H and data not shown). Therefore, the enhancement of transduction caused by As_2O_3 treatment is not unique to rAAV2 but can also be observed with several other serotypes of rAAV.

DISCUSSION

In this study, we investigated the effect of As_2O_3 on the initial transduction of rAAV vectors. We determined that As_2O_3 increased rAAV2 transduction both *in vitro* and *in vivo* and that, with As_2O_3 treatment, perinuclear accumulations of rAAV virions were maintained over time, leading to the increase in the intracellular vector genome copy numbers observed during transduction. We observed increased rAAV2 transduction with As_2O_3 at several vector doses and time points and in several cell lines with different tissue and species origins, suggesting that the effect of As_2O_3 on rAAV transduction is widespread. As the increased numbers of cells transduced correlated with an increase in vector genome copy number (Fig. 1B) and As_2O_3 had no effect on transgene

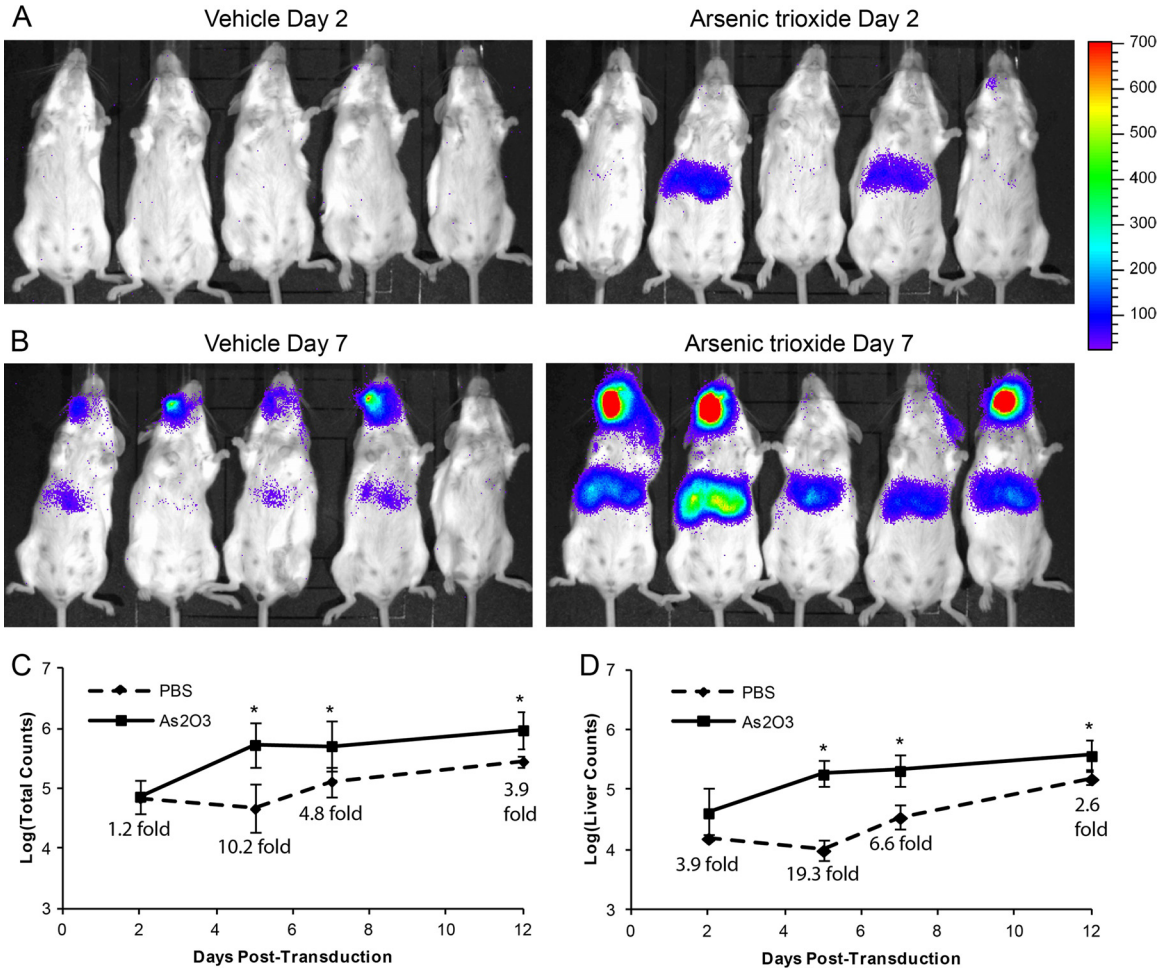

FIG 6 rAAV2 transduction effects of As_2O_3 *in vivo*. Five- to 6-week-old BALB/c mice were treated for 5 days with 5 μg/g/day As_2O_3 or a PBS vehicle control by intraperitoneal injection and transduced with 2×10^{11} vg rAAV2-CBA-luciferase on the third day of treatment. Images from luciferase live imaging at 2 days (A) and 7 days (B) posttransduction are shown (5 min of exposure). Quantification of luciferase activity from live imaging from 2 to 12 days posttransduction from the whole mouse (C) and from the area of the liver (D) is shown with fold increase values of As_2O_3 compared to those for the vehicle ($n = 5$). Error bars represent 1 SD. *, $P < 0.05$ based on the Kruskal-Wallis test.

expression independent of rAAV (data not shown), we determined that the effect of As_2O_3 on rAAV transduction occurs at a step in transduction prior to gene expression. In addition, the fold increase in rAAV transduction caused by As_2O_3 treatment was stable from 24 to 96 h posttransduction (Fig. 1C) and was observed *in vivo* in cell types which divide very slowly (Fig. 6 and 7); this suggests that the increase in transduction observed was not due to any possible difference in cell division rates, as, in this case, we would expect the difference in transduction to be minimal *in vivo* and, *in vitro*, to increase over time as vector copies were diluted in untreated cells. Furthermore, we analyzed the portion of cells in each stage of the cell cycle following As_2O_3 treatment and observed no indications of cell cycle arrest (Fig. 3D). Instead, this suggests that the difference in transduction and in intracellular genome copy number is due to a difference in the intracellular transduction pathway of rAAV. Consequently, we investigated the intracellular fate of the rAAV through both molecular and imaging techniques.

Our data demonstrate that the intracellular vector genome copy number was similar between vehicle- and As_2O_3-treated cells out to 15 to 18 h posttransduction, at which point the vector genome copy number decreased more quickly in vehicle-treated cells than in As_2O_3-treated cells (Fig. 3C). This correlates well with our confocal imaging data, which demonstrate an increased persistence of the perinuclear accumulation of rAAV virions in As_2O_3-treated cells (Fig. 4). These data suggest a model in which, in both As_2O_3-treated and untreated cells, rAAV virions enter the cell and are trafficked along microtubules to the MTOC, where they accumulate (5, 45). At the MTOC, the virions can continue their trafficking either productively by trafficking to the nucleus or nonproductively by eventually being targeted for degradation by proteasomal or lysosomal means. Without treatment, many rAAV virions are targeted for degradation, leading to relatively few virions continuing on their productive pathway (Fig. 8A). With As_2O_3 treatment, fewer virions are degraded, leading to viral stability in the perinuclear region and an increase in the productive trafficking of virions (Fig. 8B). This difference in the trafficking pathways then causes the difference in vector genome copy number and transgene expression observed.

The assertion that virions maintained at the perinuclear region

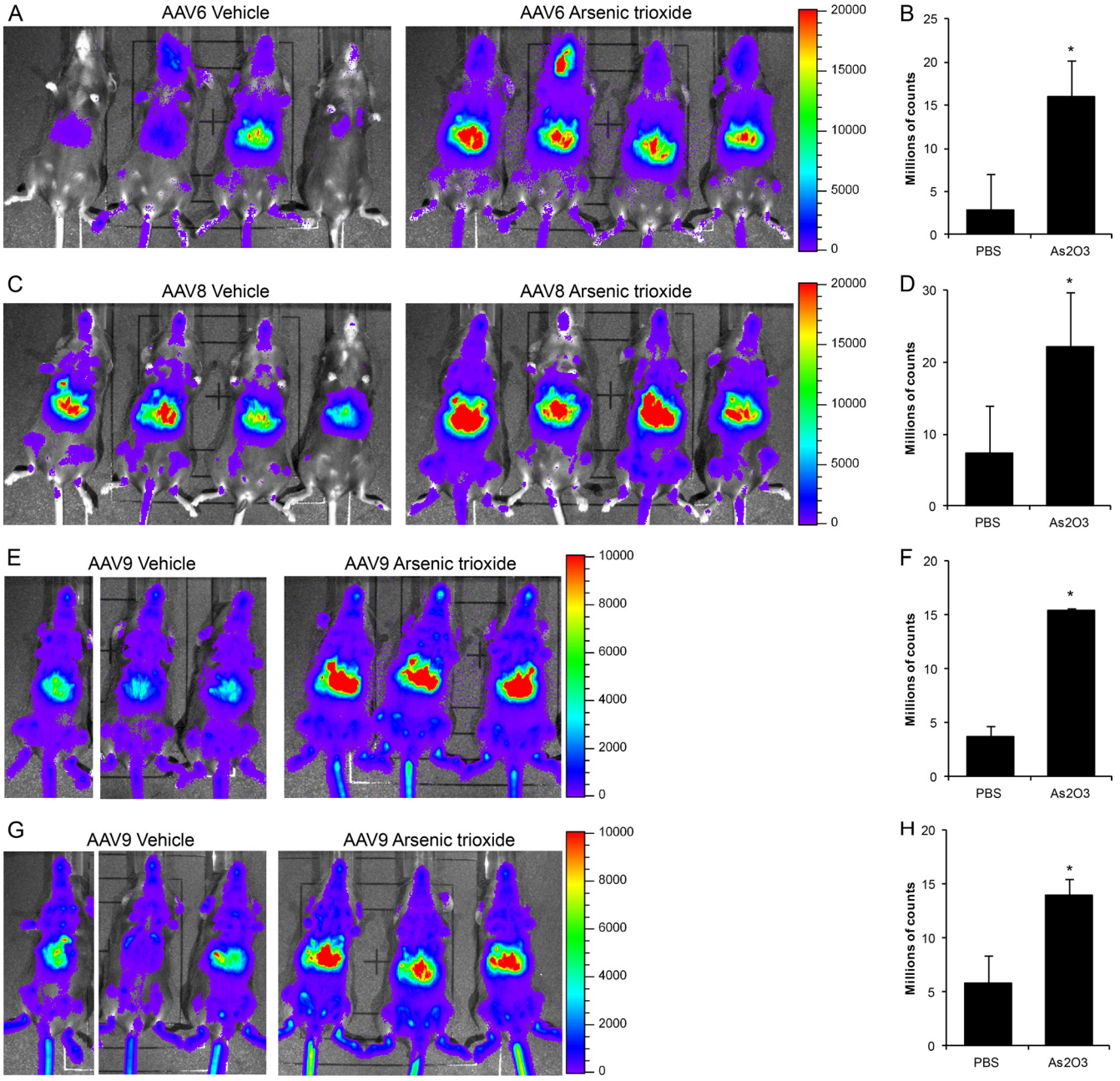

FIG 7 Transduction from several serotypes of rAAV after As_2O_3 treatment. Five- to 6-week-old C57BL/6 mice were treated for 5 days with 5 μg/g/day As_2O_3 or a PBS vehicle control by intraperitoneal injection and transduced with 1×10^{11} vg rAAV6-CBA-luciferase (A and B), rAAV8-CBA-luciferase (C and D), or rAAV9-CBA-luciferase (E, F, G, and H) on the third day of treatment. Images from live luciferase imaging are shown on day 7 for rAAV6 (A) (5 min of exposure), day 2 for rAAV8 (C) (5 min of exposure), day 5 for rAAV9 (E) (1 min of exposure), and day 21 for rAAV9 (G) (1 min of exposure). Quantification of luciferase activity from live imaging is shown at the same time points for rAAV6 (B) ($n = 4$), rAAV8 (D) ($n = 4$), and rAAV9 (F and H) ($n = 3$). Error bars represent one SD. *, $P < 0.05$ based on the Kruskal-Wallis test.

are capable of continuing their trafficking productively is supported by recent work demonstrating that the perinuclear region acts as a sink for rAAV particles and, thus, that disruption of the MTOC shortly after rAAV has accumulated can lead to increased rAAV transduction (P. J. Xaio and R. J. Samulski, unpublished data). In this study, however, we are examining later time points during which perinuclear accumulations are generally being cleared and are preventing virion degradation at the perinuclear region. Taken together, the previous work and our data suggest that maintaining the perinuclear accumulation of rAAV, rather than allowing it to be degraded over time, allows more virions to escape from this region and continue down a productive transduction pathway. In addition, previous work has suggested that rAAV virions are carried on microtubules in endosomal compartments to the MTOC, where endosomal escape presumably occurs (5). This suggests that if virions remain in the perinuclear region

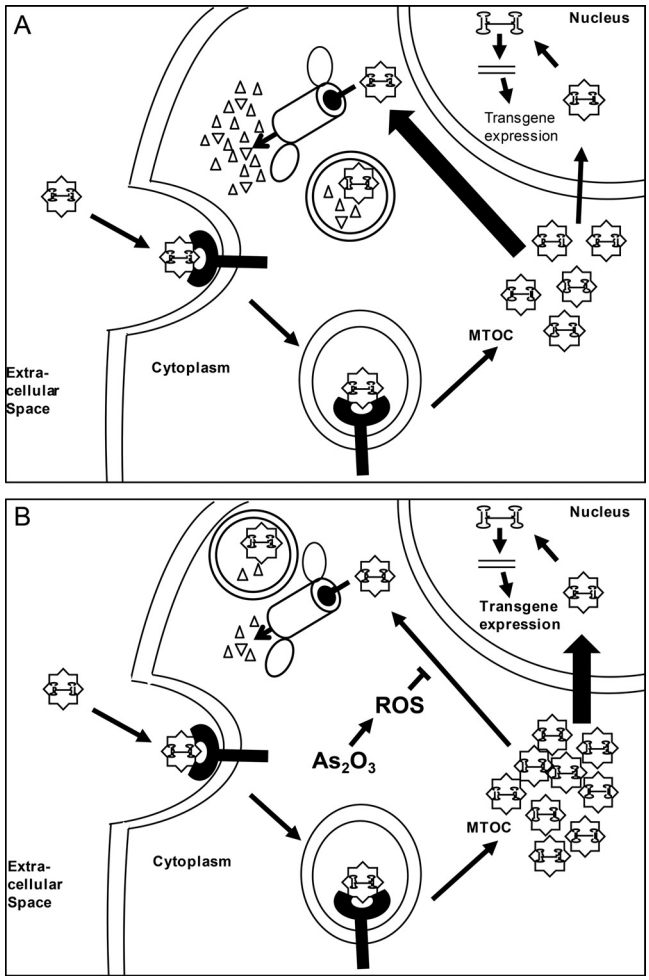

FIG 8 Model for effect of arsenic trioxide on AAV transduction. (A) In untreated cells, rAAV enters the cell through receptor-mediated endocytosis and is trafficked to the MTOC. At the MTOC, virions can be retained for a time or proceed to the nucleus; however, the majority of the virions are degraded through mechanisms possibly involving the proteasome or lysosomes, and the perinuclear accumulation clears by 32 h posttransduction. (B) In As_2O_3-treated cells, cell entry and trafficking to the MTOC occurs as described for panel A; however, As_2O_3, through ROS formation, acts to block the degradation of the virion. Consequently, more virions continue on in the transduction pathway, ultimately leading to greater transgene expression.

for longer periods of time, more virions can be released from endosomes and escape perinuclear retention to continue on a productive trafficking pathway to the nucleus.

Proteasome inhibitors, such as MG132, have previously been demonstrated to lead to increased nucleolar accumulation of rAAV virions and to increased intracellular vector genome copy number, leading to higher transduction (6). Given the probable role of degradation in the effect of As_2O_3 on rAAV transduction, we find it interesting that As_2O_3 and MG132 have at least partially independent effects on rAAV transduction (Fig. 3E) and appear to act at different levels on the intracellular trafficking of rAAV (Fig. 4) (6). This suggests the following possibilities: (i) rAAV virions are being degraded in significant numbers by a nonproteasomal mechanism that As_2O_3 affects, leading to the separate roles of MG132 and As_2O_3; (ii) MG132 increases rAAV transduction through a mechanism that is separate from inhibition of the proteasome, so the decrease in degradation observed with As_2O_3 is separated from that of MG132; or (iii) MG132 and As_2O_3 each have partial effects on the proteasomal degradation of rAAV in separate steps in intracellular trafficking, perhaps in perinuclear degradation for As_2O_3 and in nuclear degradation for MG132, leading to their separate effects. We are currently investigating the specific mechanisms of rAAV degradation modified with As_2O_3 treatment, which should lend clarity to these issues.

In addition to rAAV2, we investigated the ability of As_2O_3 to enhance the transduction of several other rAAV serotypes *in vivo*. As_2O_3 enhanced the transduction of rAAV6, rAAV8, and rAAV9 *in vivo* early after transduction (Fig. 7); however, the kinetics of the enhancement varied based on the serotype. Specifically, As_2O_3 enhanced the transduction of rAAV2 and rAAV9 at time points ranging from 2 days posttransduction to 14 days or more posttransduction, while rAAV8's transduction is enhanced at 2 days posttransduction but not at later time points (Fig. 6 and 7 and data not shown). This is interesting, as it suggests that there is capsid specificity in the response to As_2O_3, perhaps derived from differences in intracellular trafficking patterns or efficiencies with different serotypes. Although the intracellular trafficking of rAAV2 is the most thoroughly studied, several reports have begun to compare the trafficking pathways of different rAAV serotypes. For instance, rAAV1 and rAAV5 can traffic to the nucleus of HeLa cells more quickly than rAAV2 but have lower levels of transduction due to either poor uncoating or rapid degradation, respectively (49). In addition, a recent report suggested that, perhaps due to differences in receptor usage, rAAV2 and rAAV8 differentially traffic through endosomal compartments and have different requirements for endosomal escape (50). Specifically, rAAV2 is reported to traffic through early, recycling, and late endosomes and to require low pH for endosomal escape, while rAAV8 does not traffic through late endosomes, only early and recycling endosomes, and low pH is not sufficient for its endosomal escape. The difference in the kinetics of As_2O_3's effect on the transduction of rAAV2 and rAAV8 suggests a role for endosomal trafficking in the As_2O_3 effect. Determining the role of endosomes in As_2O_3's transduction effect and determining the specific regions of the capsid responsible for the differences in the As_2O_3 effect will be interesting avenues to pursue in the future.

As_2O_3 has well-known effects on cellular concentrations of ROS, and ROS are thought to act as intermediates in some of As_2O_3's other cellular effects; therefore, we investigated whether the effects of As_2O_3 on rAAV2 transduction were mediated through ROS formation. We determined that As_2O_3 causes a dose-dependent increase in ROS that corresponds well to the dose-dependent increase in rAAV2 transduction, and that inhibiting the formation of ROS inhibits As_2O_3's enhancement of rAAV2 transduction (Fig. 5). Interestingly, ROS formation has previously been demonstrated to be important for enhancement of rAAV transduction by hydroxyurea and UV light, and a role for second-strand DNA synthesis was suggested (8, 51), although later reports questioned this assertion (6, 52). As we determined that As_2O_3 can enhance the transduction of self-complementary rAAV2 (Fig. 3A), which does not require second-strand synthesis, and also observed changes in earlier steps in transduction (Fig. 4), it is unlikely that As_2O_3 is acting through enhancement of second-strand synthesis. Furthermore, although hydroxyurea acts through ROS, similar to As_2O_3, it increases the nuclear localization of rAAV2 without increasing the intracellular vector genome

copy number (6), whereas As_2O_3 increases vector genome copy number (Fig. 1B) and acts at an earlier step in transduction (Fig. 4). This suggests that, depending on the initiator, ROS can act on several different steps in rAAV's transduction pathway. In this case, ROS may have a broad role in a number of steps in AAV's life cycle.

As_2O_3 has many effects on the cellular level involving ROS formation, which may play a role in its enhancement of rAAV transduction. For instance, As_2O_3 has been shown to inhibit NF-κB activation by directly binding a cysteine residue on the activation loop of the protein (29); however, as the concentration of As_2O_3 necessary to inhibit NF-κB activation was higher than those used in our studies and the timing of As_2O_3 addition was different, the status of NF-κB activation in our experiments is unclear. Several studies have suggested a positive role for NF-κB activation in rAAV transduction (52, 53), and several other ROS generators, such as UV light and H_2O_2, have been shown to increase NF-κB activation, although this activation was not necessary for their effects on AAV transduction (51, 52). Nevertheless, it will be enlightening to explore the role of NF-κB in As_2O_3-mediated enhancement of rAAV transduction further. Another effect of As_2O_3 and ROS is to degrade the promyelocytic leukemia protein (30), which has well-known cell-intrinsic antiviral activities against many different viruses (reviewed in reference 54). However, we observed an increase in rAAV2 transduction with no apparent change in PML levels or localization, and we observed an increase in transduction in the absence of PML (data not shown). These data suggest that PML is not a key factor in the effect of As_2O_3 on rAAV transduction. Therefore, identification of the specific cellular mechanisms responsible for the enhancement of rAAV transduction upon As_2O_3 treatment will continue to be an interesting avenue of research.

As_2O_3 has several known effects on other viruses, either inhibiting or enhancing their replication. As_2O_3 strongly inhibits hepatitis C virus replication through a mechanism that involves ROS but is independent of PML (55, 56); although the specific mechanism has not been elucidated, this is interesting, as As_2O_3's enhancement of rAAV transduction is also mediated by ROS and is independent of PML. Moreover, the replication of several other viruses is enhanced by As_2O_3 treatment. As_2O_3 causes an enhancement of HIV replication only in nonpermissive cell types in a manner that depends on the expression of TRIM5α and APOBEC3G (35, 36). It is noteworthy that the effects of As_2O_3 on HIV are cell line specific, while the effects on AAV are more general, and that As_2O_3 acts on HIV through two cellular proteins which are unlikely to, or are known not to, interact with AAV (57). This suggests that although As_2O_3 has effects on several viruses, the effects are caused by widespread, diverse mechanisms.

Interestingly, several lines of evidence have suggested that trivalent arsenic can induce lytic replication in alphaherpesviruses (HSV and VZV), betaherpesviruses (human cytomegalovirus [HCMV]), and gammaherpesviruses (Epstein-Barr virus [EBV]) (37, 38, 58, 59). Specifically, reactivation of HSV and VZV has been observed in acute promyelocytic leukemia patients treated with As_2O_3 at a rate higher than that found with general immunosuppression and in a manner which is not consistent with reactivation from immunosuppression (37, 38). To our knowledge, no studies have been published investigating the mechanism for the reactivation of HSV or VZV in response to As_2O_3. However, activation of EBV replication in response to As_2O_3 was correlated with the degradation of PML, although no direct evidence of a link was presented (59), while the induction of HCMV immediate-early gene synthesis by sodium arsenite, another trivalent arsenic compound, was suggested to be the result of heat shock protein activation (58). Overall, the mechanisms for herpesvirus reactivation following As_2O_3 treatment remain incompletely understood, and delving into the mechanisms by which As_2O_3 enhances the replication of other viruses may lead to useful insights into herpesvirus reactivation. For instance, as cellular degradation pathways may play a role in the enhancement of rAAV2 transduction by As_2O_3, it would be interesting to determine whether there is a role for these pathways in As_2O_3-mediated reactivation of HSV or VZV.

In addition to elucidating possible mechanisms to explore the effect of As_2O_3 on the replication of other viruses, the enhancement of rAAV transduction observed with As_2O_3 treatment may become important for gene therapy applications. We observed an increase in rAAV2 transduction both *in vitro* (Fig. 1 and 2) and *in vivo* in several serotypes of rAAV with no apparent toxicity (Fig. 6 and 7 and data not shown). For some gene therapy applications, especially those involving systemic gene delivery, low levels of transgene expression or loss of transgene expression over time have limited the efficacy observed in clinical settings (60, 61). Pharmacological treatments are a promising approach to increasing rAAV transduction in order to address these issues, particularly when pharmacological agents currently approved for use in humans are utilized. In fact, bortezomib, a proteasome inhibitor, has been used in large-animal models to enhance rAAV transduction (17); however, the serious and even fatal side effects associated with this drug makes its clinical use for enhancement of rAAV transduction problematic (17, 22). For this reason, identifying other agents, such as As_2O_3, capable of enhancing rAAV transduction is important to the clinical applications of rAAV. In addition, investigating the mechanism behind the increase in transduction observed with pharmacological treatments may allow us to identify steps in transduction or cellular factors which limit rAAV transduction and to design other strategies to circumvent these difficulties. Therefore, our data demonstrating that As_2O_3 increases the transduction of rAAV vectors both *in vitro* and *in vivo* and suggesting that it acts to stabilize perinuclear accumulations of rAAV in a way that is dependent on ROS may broaden our toolkit for understanding AAV biology and improving its gene therapy applications. In conclusion, pursuing the biology behind the effects of As_2O_3 on rAAV transduction may have important implications both for AAV-mediated gene therapy and for elucidating the mechanism by which As_2O_3 affects the replication of other clinically relevant viruses.

ACKNOWLEDGMENTS

This work was supported by National Institutes of Health grants 1R01AI080726 and 5R01DK084033 (to C.L. and R.J.S.), 5U54AR056953 and 5R01AI072176 (to R.J.S.), and fellowship 5T32-AI007419 (to A.M.M.).

We thank the members of the University of North Carolina at Chapel Hill Gene Therapy Center for productive discussions, particularly Sarah Nicolson, Matthew Hirsch, and Jayme Warischalk. We thank Kenton Woodard for the use of his self-complementary vector and Swati Yadav and Sophia Shih for determining the titers of AAV vectors by qPCR. Equipment and software from the UNC Flow Cytometry Core, UNC Microscopy Services Laboratory, and the UNC Small Animal Imaging Facility were used in this study.

REFERENCES

1. **Nakai H, Yant SR, Storm TA, Fuess S, Meuse L, Kay MA.** 2001. Extrachromosomal recombinant adeno-associated virus vector genomes are primarily responsible for stable liver transduction in vivo. J. Virol. **75**:6969–6976.
2. **Xiao X, Xiao W, Li J, Samulski RJ.** 1997. A novel 165-base-pair terminal repeat sequence is the sole cis requirement for the adeno-associated virus life cycle. J. Virol. **71**:941–948.
3. **Mitchell AM, Nicolson SC, Warischalk JK, Samulski RJ.** 2010. AAV's anatomy: roadmap for optimizing vectors for translational success. Curr. Gene Ther. **10**:319–340.
4. **Bartlett JS, Wilcher R, Samulski RJ.** 2000. Infectious entry pathway of adeno-associated virus and adeno-associated virus vectors. J. Virol. **74**: 2777–2785.
5. **Xiao PJ, Samulski RJ.** 2012. Cytoplasmic trafficking, endosomal escape, and perinuclear accumulation of adeno-associated virus type 2 particles are facilitated by microtubule network. J. Virol. **86**:10462–10473.
6. **Johnson JS, Samulski RJ.** 2009. Enhancement of adeno-associated virus infection by mobilizing capsids into and out of the nucleolus. J. Virol. **83**:2632–2644.
7. **Xiao W, Warrington KH, Jr, Hearing P, Hughes J, Muzyczka N.** 2002. Adenovirus-facilitated nuclear translocation of adeno-associated virus type 2. J. Virol. **76**:11505–11517.
8. **Ferrari FK, Samulski T, Shenk T, Samulski RJ.** 1996. Second-strand synthesis is a rate-limiting step for efficient transduction by recombinant adeno-associated virus vectors. J. Virol. **70**:3227–3234.
9. **McCarty DM, Fu H, Monahan PE, Toulson CE, Naik P, Samulski RJ.** 2003. Adeno-associated virus terminal repeat (TR) mutant generates self-complementary vectors to overcome the rate-limiting step to transduction in vivo. Gene Ther. **10**:2112–2118.
10. **Johnson JS, Gentzsch M, Zhang L, Ribeiro CM, Kantor B, Kafri T, Pickles RJ, Samulski RJ.** 2011. AAV exploits subcellular stress associated with inflammation, endoplasmic reticulum expansion, and misfolded proteins in models of cystic fibrosis. PLoS Pathog. **7**:e1002053. doi:10.1371/journal.ppat.1002053.
11. **Zhong L, Qing K, Si Y, Chen L, Tan M, Srivastava A.** 2004. Heat-shock treatment-mediated increase in transduction by recombinant adeno-associated virus 2 vectors is independent of the cellular heat-shock protein 90. J. Biol. Chem. **279**:12714–12723.
12. **Yalkinoglu AO, Heilbronn R, Burkle A, Schlehofer JR, Hausen H.** 1988. DNA amplification of adeno-associated virus as a response to cellular genotoxic stress. Cancer Res. **48**:3123–3129.
13. **Golding I.** 2011. Decision making in living cells: lessons from a simple system. Annu. Rev. Biophys. **40**:63–80.
14. **van der Ven A, van Diest R, Hamulyak K, Maes M, Bruggeman C, Appels A.** 2003. Herpes viruses, cytokines, and altered hemostasis in vital exhaustion. Psychosom. Med. **65**:194–200.
15. **Huang W, Xie P, Xu M, Li P, Zao G.** 2011. The influence of stress factors on the reactivation of latent herpes simplex virus type 1 in infected mice. Cell Biochem. Biophys. **61**:115–122.
16. **Douar AM, Poulard K, Stockholm D, Danos O.** 2001. Intracellular trafficking of adeno-associated virus vectors: routing to the late endosomal compartment and proteasome degradation. J. Virol. **75**:1824–1833.
17. **Monahan PE, Lothrop CD, Sun J, Hirsch ML, Kafri T, Kantor B, Sarkar R, Tillson DM, Elia JR, Samulski RJ.** 2010. Proteasome inhibitors enhance gene delivery by AAV virus vectors expressing large genomes in hemophilia mouse and dog models: a strategy for broad clinical application. Mol. Ther. **18**:1907–1916.
18. **Russell DW, Alexander IE, Miller AD.** 1995. DNA synthesis and topoisomerase inhibitors increase transduction by adeno-associated virus vectors. Proc. Natl. Acad. Sci. U. S. A. **92**:5719–5723.
19. **Duan D, Yue Y, Yan Z, Yang J, Engelhardt JF.** 2000. Endosomal processing limits gene transfer to polarized airway epithelia by adeno-associated virus. J. Clin. Investig. **105**:1573–1587.
20. **Ju XD, Lou SQ, Wang WG, Peng JQ, Tian H.** 2004. Effect of hydroxyurea and etoposide on transduction of human bone marrow mesenchymal stem and progenitor cell by adeno-associated virus vectors. Acta Pharmacol. Sin. **25**:196–202.
21. **Prasad KM, Xu Y, Yang Z, Toufektsian MC, Berr SS, French BA.** 2007. Topoisomerase inhibition accelerates gene expression after adeno-associated virus-mediated gene transfer to the mammalian heart. Mol. Ther. **15**:764–771.
22. **Cornelis T, Beckers EA, Driessen AL, van der Sande FM, Koek GH.** 2012. Bortezomib-associated fatal liver failure in a haemodialysis patient with multiple myeloma. Clin. Toxicol. **50**:444–445.
23. **Au WY, Kumana CR, Lee HK, Lin SY, Liu H, Yeung DY, Lau JS, Kwong YL.** 2011. Oral arsenic trioxide-based maintenance regimens for first complete remission of acute promyelocytic leukemia: a 10-year follow-up study. Blood **118**:6535–6543.
24. **Park WH, Seol JG, Kim ES, Hyun JM, Jung CW, Lee CC, Kim BK, Lee YY.** 2000. Arsenic trioxide-mediated growth inhibition in MC/CAR myeloma cells via cell cycle arrest in association with induction of cyclin-dependent kinase inhibitor, p21, and apoptosis. Cancer Res. **60**:3065–3071.
25. **List A, Beran M, DiPersio J, Slack J, Vey N, Rosenfeld CS, Greenberg P.** 2003. Opportunities for trisenox (arsenic trioxide) in the treatment of myelodysplastic syndromes. Leukemia **17**:1499–1507.
26. **Baljevic M, Park JH, Stein E, Douer D, Altman JK, Tallman MS.** 2011. Curing all patients with acute promyelocytic leukemia: are we there yet? Hematol. Oncol. Clin. North Am. **25**:1215–1233.
27. **Spuches AM, Kruszyna HG, Rich AM, Wilcox DE.** 2005. Thermodynamics of the As(III)-thiol interaction: arsenite and monomethylarsenite complexes with glutathione, dihydrolipoic acid, and other thiol ligands. Inorg. Chem. **44**:2964–2972.
28. **Dai J, Weinberg RS, Waxman S, Jing Y.** 1999. Malignant cells can be sensitized to undergo growth inhibition and apoptosis by arsenic trioxide through modulation of the glutathione redox system. Blood **93**:268–277.
29. **Kapahi P, Takahashi T, Natoli G, Adams SR, Chen Y, Tsien RY, Karin M.** 2000. Inhibition of NF-kappa B activation by arsenite through reaction with a critical cysteine in the activation loop of Ikappa B kinase. J. Biol. Chem. **275**:36062–36066.
30. **Jeanne M, Lallemand-Breitenbach V, Ferhi O, Koken M, Le Bras M, Duffort S, Peres L, Berthier C, Soilihi H, Raught B, de The H.** 2010. PML/RARA oxidation and arsenic binding initiate the antileukemia response of As2O3. Cancer Cell **18**:88–98.
31. **Larochette N, Decaudin D, Jacotot E, Brenner C, Marzo I, Susin SA, Zamzami N, Xie Z, Reed J, Kroemer G.** 1999. Arsenite induces apoptosis via a direct effect on the mitochondrial permeability transition pore. Exp. Cell Res. **249**:413–421.
32. **Hong SH, Yang Z, Privalsky ML.** 2001. Arsenic trioxide is a potent inhibitor of the interaction of SMRT corepressor with Its transcription factor partners, including the PML-retinoic acid receptor alpha oncoprotein found in human acute promyelocytic leukemia. Mol. Cell. Biol. **21**: 7172–7182.
33. **Park JW, Choi YJ, Jang MA, Baek SH, Lim JH, Passaniti T, Kwon TK.** 2001. Arsenic trioxide induces G2/M growth arrest and apoptosis after caspase-3 activation and bcl-2 phosphorylation in promonocytic U937 cells. Biochem. Biophys. Res. Commun. **286**:726–734.
34. **Malbec M, Pham QT, Plourde MB, Letourneau-Hogan A, Nepveu-Traversy ME, Berthoux L.** 2010. Murine double minute 2 as a modulator of retroviral restrictions mediated by TRIM5alpha. Virology **405**:414–423.
35. **Sebastian S, Sokolskaja E, Luban J.** 2006. Arsenic counteracts human immunodeficiency virus type 1 restriction by various TRIM5 orthologues in a cell type-dependent manner. J. Virol. **80**:2051–2054.
36. **Stalder R, Blanchet F, Mangeat B, Piguet V.** 2010. Arsenic modulates APOBEC3G-mediated restriction to HIV-1 infection in myeloid dendritic cells. J. Leukoc. Biol. **88**:1251–1258.
37. **Au WY, Kwong YL.** 2005. Frequent varicella zoster reactivation associated with therapeutic use of arsenic trioxide: portents of an old scourge. J. Am. Acad. Dermatol. **53**:890–892.
38. **Nouri K, Ricotti CA, Jr, Bouzari N, Chen H, Ahn E, Bach A.** 2006. The incidence of recurrent herpes simplex and herpes zoster infection during treatment with arsenic trioxide. J. Drugs Dermatol. **5**:182–185.
39. **Jennings K, Miyamae T, Traister R, Marinov A, Katakura S, Sowders D, Trapnell B, Wilson JM, Gao G, Hirsch R.** 2005. Proteasome inhibition enhances AAV-mediated transgene expression in human synoviocytes in vitro and in vivo. Mol. Ther. **11**:600–607.
40. **Grieger JC, Choi VW, Samulski RJ.** 2006. Production and characterization of adeno-associated viral vectors. Nat. Protoc. **1**:1412–1428.
41. **Zhang W, Ohnishi K, Shigeno K, Fujisawa S, Naito K, Nakamura S, Takeshita K, Takeshita A, Ohno R.** 1998. The induction of apoptosis and cell cycle arrest by arsenic trioxide in lymphoid neoplasms. Leukemia **12**:1383–1391.
42. **Xiao PJ, Li C, Neumann A, Samulski RJ.** 2012. Quantitative 3D tracing

of gene-delivery viral vectors in human cells and animal tissues. Mol. Ther. **20**:317–328.
43. **Gu Y, Lewis DF, Zhang Y, Groome LJ, Wang Y.** 2006. Increased superoxide generation and decreased stress protein Hsp90 expression in human umbilical cord vein endothelial cells (HUVECs) from pregnancies complicated by preeclampsia. Hypertens. Pregnancy **25**:169–182.
44. **Li C, Diprimio N, Bowles DE, Hirsch ML, Monahan PE, Asokan A, Rabinowitz J, Agbandje-McKenna M, Samulski RJ.** 2012. Single amino acid modification of adeno-associated virus capsid changes transduction and humoral immune profiles. J. Virol. **86**:7752–7759.
45. **Sanlioglu S, Benson PK, Yang J, Atkinson EM, Reynolds T, Engelhardt JF.** 2000. Endocytosis and nuclear trafficking of adeno-associated virus type 2 are controlled by rac1 and phosphatidylinositol-3 kinase activation. J. Virol. **74**:9184–9196.
46. **Miller WH, Jr, Schipper HM, Lee JS, Singer J, Waxman S.** 2002. Mechanisms of action of arsenic trioxide. Cancer Res. **62**:3893–3903.
47. **Lallemand-Breitenbach V, Guillemin MC, Janin A, Daniel MT, Degos L, Kogan SC, Bishop JM, de The H.** 1999. Retinoic acid and arsenic synergize to eradicate leukemic cells in a mouse model of acute promyelocytic leukemia. J. Exp. Med. **189**:1043–1052.
48. **Shen ZX, Chen GQ, Ni JH, Li XS, Xiong SM, Qiu QY, Zhu J, Tang W, Sun GL, Yang KQ, Chen Y, Zhou L, Fang ZW, Wang YT, Ma J, Zhang P, Zhang TD, Chen SJ, Chen Z, Wang ZY.** 1997. Use of arsenic trioxide (As2O3) in the treatment of acute promyelocytic leukemia (APL): II. Clinical efficacy and pharmacokinetics in relapsed patients. Blood **89**:3354–3360.
49. **Keiser NW, Yan Z, Zhang Y, Lei-Butters DC, Engelhardt JF.** 2011. Unique characteristics of AAV1, 2, and 5 viral entry, intracellular trafficking, and nuclear import define transduction efficiency in HeLa cells. Hum. Gene Ther. **22**:1433–1444.
50. **Liu Y, Joo KI, Wang P.** 2012. Endocytic processing of adeno-associated virus type 8 vectors for transduction of target cells. Gene Ther. doi:10.1038/gt.2012.41. [Epub ahead of print.]
51. **Sanlioglu S, Engelhardt JF.** 1999. Cellular redox state alters recombinant adeno-associated virus transduction through tyrosine phosphatase pathways. Gene Ther. **6**:1427–1437.
52. **Wheeler MD, Kono H, Rusyn I, Arteel GE, McCarty D, Samulski RJ, Thurman RG.** 2000. Chronic ethanol increases adeno-associated viral transgene expression in rat liver via oxidant and NFkappaB-dependent mechanisms. Hepatology **32**:1050–1059.
53. **Jayandharan GR, Aslanidi G, Martino AT, Jahn SC, Perrin GQ, Herzog RW, Srivastava A.** 2011. Activation of the NF-kappaB pathway by adeno-associated virus (AAV) vectors and its implications in immune response and gene therapy. Proc. Natl. Acad. Sci. U. S. A. **108**:3743–3748.
54. **Geoffroy MC, Chelbi-Alix MK.** 2011. Role of promyelocytic leukemia protein in host antiviral defense. J. Interferon Cytokine Res. **31**:145–158.
55. **Hwang DR, Tsai YC, Lee JC, Huang KK, Lin RK, Ho CH, Chiou JM, Lin YT, Hsu JT, Yeh CT.** 2004. Inhibition of hepatitis C virus replication by arsenic trioxide. Antimicrob. Agents Chemother. **48**:2876–2882.
56. **Kuroki M, Ariumi Y, Ikeda M, Dansako H, Wakita T, Kato N.** 2009. Arsenic trioxide inhibits hepatitis C virus RNA replication through modulation of the glutathione redox system and oxidative stress. J. Virol. **83**:2338–2348.
57. **Bulliard Y, Narvaiza I, Bertero A, Peddi S, Rohrig UF, Ortiz M, Zoete V, Castro-Diaz N, Turelli P, Telenti A, Michielin O, Weitzman MD, Trono D.** 2011. Structure-function analyses point to a polynucleotide-accommodating groove essential for APOBEC3A restriction activities. J. Virol. **85**:1765–1776.
58. **Geelen JL, Boom R, Klaver GP, Minnaar RP, Feltkamp MC, van Milligen FJ, Sol CJ, van der Noordaa J.** 1987. Transcriptional activation of the major immediate early transcription unit of human cytomegalovirus by heat-shock, arsenite and protein synthesis inhibitors. J. Gen. Virol. **68**(Pt 11):2925–2931.
59. **Sides MD, Block GJ, Shan B, Esteves KC, Lin Z, Flemington EK, Lasky JA.** 2011. Arsenic mediated disruption of promyelocytic leukemia protein nuclear bodies induces ganciclovir susceptibility in Epstein-Barr positive epithelial cells. Virology **416**:86–97.
60. **Manno CS, Pierce GF, Arruda VR, Glader B, Ragni M, Rasko JJ, Ozelo MC, Hoots K, Blatt P, Konkle B, Dake M, Kaye R, Razavi M, Zajko A, Zehnder J, Rustagi PK, Nakai H, Chew A, Leonard D, Wright JF, Lessard RR, Sommer JM, Tigges M, Sabatino D, Luk A, Jiang H, Mingozzi F, Couto L, Ertl HC, High KA, Kay MA.** 2006. Successful transduction of liver in hemophilia by AAV-factor IX and limitations imposed by the host immune response. Nat. Med. **12**:342–347.
61. **Nathwani AC, Tuddenham EG, Rangarajan S, Rosales C, McIntosh J, Linch DC, Chowdary P, Riddell A, Pie AJ, Harrington C, O'Beirne J, Smith K, Pasi J, Glader B, Rustagi P, Ng CY, Kay MA, Zhou J, Spence Y, Morton CL, Allay J, Coleman J, Sleep S, Cunningham JM, Srivastava D, Basner-Tschakarjan E, Mingozzi F, High KA, Gray JT, Reiss UM, Nienhuis AW, Davidoff AM.** 2011. Adenovirus-associated virus vector-mediated gene transfer in hemophilia B. N. Engl. J. Med. **365**:2357–2365.